



## MEASUREMENT BASED INVESTIGATION OF CYCLOSTATIONARITY OF OFDMA SIGNALS



Kürşat TEKBIYIK<sup>1</sup>, Hakan ALAKOCA<sup>1</sup>, H. Bahadır Tuğrel<sup>1</sup>, Cem AYYILDIZ<sup>2</sup>,  
Güneş KARABULUT KURT<sup>1</sup>

<sup>1</sup>Istanbul Technical University, Istanbul, Turkey

<sup>2</sup>Turkcell Communication Services, Istanbul, Turkey

tekbiiyk@itu.edu.tr, alakoca@itu.edu.tr, tugrel@itu.edu.tr, cem.ayyildiz@gmail.com, gkurt@itu.edu.tr

**Abstract:** Increasing need for efficient usage of frequency spectrum fosters the search of new methods. Network operators are forced to use their frequency band as efficiently as possible due to high subscriber demands. Blind identification of unauthorized users becomes necessary to obtain efficient usage of frequency bands. Like cyclic prefix (CP) length, the position of the zero padding in the frame has an impact on the cyclostationary characteristics of signal, that can be used for blind identification of unauthorized users. In this paper, it is shown that signals from two different users with the same CP lengths can be differentiated from each other via measurement results. Cyclic autocorrelation function and spectral correlation density function are computed for each user. The differences between their cyclic properties are shown by software defined radio measurements. It is shown that signals transmitted from specific users can be differentiated by using cyclic autocorrelation and spectral density functions characteristics.

**Keywords:** OFDMA, cyclostationarity, blind recognition, software defined radio

### 1. Introduction

The need for frequency spectrum is constantly increasing. The customers demand high data transmission speeds and wide coverage areas. To satisfy their requests, operators try to expand their frequency bands, which is not a easy or a cheap option. They must find effective new ways to accommodate the increasing demands of subscribers. As the frequency spectrum is already limited, reduction of the data transmission speed and coverage area due to interference can not be accepted. It is important to develop methods to monitor efficient usage of the limited electromagnetic spectrum against such cases. In addition, unlicensed spectrum equipment also reduces the efficiency.

In our previous study [1], it was shown via simulations that orthogonal frequency division multiplexed (OFDM) symbols with different cyclic prefix (CP) lengths could be separated from each other to blindly differentiate network users. In this paper, identification of different users with OFDM symbols of the same CP length is investigated. It is aimed to blindly differentiate a desired message signal. Cyclostationarity properties are investigated in terms of cyclic autocorrelation function (CAF) and spectral correlation density (SCD) function. To determine the performances of the considered techniques a software defined radio (SDR) based testbed is designed and developed. Two different users' orthogonal frequency division multiple access (OFDMA) signals, that have same CP symbol lengths, are generated by using two SDR nodes, specifically Universal Software Radio Peripheral (USRP) 2921 nodes. These generated signals are received by an SDR and their CAF and fast Fourier transform (FFT)

of CAF, SCD function, are computed. It is shown that the cyclostationary features of a signal vary with zero padding position in the frame; thus, the cyclostationary feature differences between OFDMA signals which are received from two distinct users -even if with same CP length- can be blindly identified.

### 2. Related Literature

There are various studies in the field of cyclostationarity signal analysis. Using cyclostationary signal features, blind detection and spectrum sensing methods are proposed. In [2, 3] the modulation scheme is determined by using cyclostationary signal analysis. An algorithm is proposed for detection of primary user signals in colored Gaussian noise by using cognitive radios in [4]. This algorithm uses conjugate and non-conjugate CAF. Pilot-based and CP-based cyclostationary analysis are detailed in [5] for Wi-Fi signals. In [6], the USRP platform and SCD function are used for recognition of RF signals. In [7], cyclostationary signal analysis is detailed for signals using the same frequency band causing interference. A method decreasing computational complexity is stated in [8]. The method is based on eigenvalue matrix for fractional low order cyclostationarity. It is stated that this method shows better detection performance than common cyclostationary detectors. In [9], the detection of undefined secondary users is studied by using time smoothing method. Also, [10] is an informative source for implementations of digital spectral correlation analyzers.

In our previous studies [1, 11], the impact of CP length on the cyclostationary features of signals and the difference between jamming signal and OFDMA signals

are shown, respectively. In this paper, we aim to differentiate the signals using the same protocol with the same CP length. CAFs and SCD functions are given for different signals of two users.

### 3. Cyclostationarity

Many frequently used signals are not stationary, but they are processed as if they were stationary. Hence, some periodicities or characteristics are ignored by signal processors. To improve the performances of signal processors, random signals can be modeled with statistical parameters periodically varying in the time domain. This model is referred to as cyclostationarity model. The processors can bring underlying features of signals by utilizing cyclostationarity.

To obtain second-order cyclostationarity, a nonlinear transform is employed for continuous signal  $x(t)$  as

$$y_\tau(t) = x(t + \tau/2)x^*(t - \tau/2). \quad (1)$$

Fourier coefficients of  $y_\tau(t)$  is

$$M_y^\alpha = \langle y_\tau(t)e^{-i2\pi\alpha t} \rangle, \quad (2)$$

where  $\langle \cdot \rangle$  is the time averaging operation. Therefore, the Fourier coefficients of (1) are obtained as

$$R_x^\alpha(\tau) = \langle x(t + \tau/2)x^*(t - \tau/2)e^{-i2\pi\alpha t} \rangle. \quad (3)$$

Two different weighting factor such as  $e^{-i\pi\alpha(t-\frac{\tau}{2})}$  and  $e^{i\pi\alpha(t+\frac{\tau}{2})}$  can be used and (3) can be rewritten to obtain CAF as

$$R_x^\alpha(\tau) = \langle [x(t + \frac{\tau}{2})e^{-i\pi\alpha(t+\frac{\tau}{2})}] [x^*(t - \frac{\tau}{2})e^{-i\pi\alpha(t-\frac{\tau}{2})}] \rangle. \quad (4)$$

Let us define  $u(t) = x(t)e^{-i\pi\alpha t}$  and  $v(t) = x(t)e^{i\pi\alpha t}$ . It should be remembered that multiplying with  $e^{\pm i2\pi\alpha t}$  results in  $\pm\alpha$  shift in frequency domain. Therefore,

$$U(f) = X(f + \frac{\alpha}{2}) \text{ and } V(f) = X(f - \frac{\alpha}{2}). \quad (5)$$

If and only if the correlation between  $u(t)$  and  $v(t)$  is not zero, we can say that  $R_x^\alpha(\tau)$  contains second-order periodicity.  $\alpha$  is called cyclic frequency.

The frequency domain can provide a more reliable representation for communication applications. Thus, SCD function can be employed instead of CAF. While the average power of a stationary signal  $x(t)$  is equal to  $\langle |x(t)|^2 \rangle = R_x(0)$ ,  $\langle u(t)v^*(t) \rangle$  indicates  $R_x^\alpha(0) = \langle |x(t)|^2 e^{-i2\pi\alpha t} \rangle$  of cyclostationary signal  $x(t)$ . To measure the average power of received signal at the output of the filter, the signal  $x(t)$  is passed through a narrowband bandpass filter (BPF) with bandwidth  $B$ . Let us assume  $B$  is approaching zero and many filters are employed. In this

case, the set of average power of outputs express the power spectral density (PSD) as

$$S_x(f) = \lim_{B \rightarrow 0} \frac{1}{B} \langle |h_B^f(t) * x(t)|^2 \rangle, \quad (6)$$

where  $h_B^f(t)$  is the impulse response of the one-sided filter with bandwidth  $B$  and center frequency  $f$ . We can rewrite (9) in terms of  $u(t)$  and  $v(t)$  like this

$$S_x^\alpha(f) = \lim_{B \rightarrow 0} \frac{1}{B} \langle [h_B^f(t) * u(t)][h_B^f(t) * v(t)]^* \rangle. \quad (7)$$

(7) generates the spectral density of correlation between  $X(f - \frac{\alpha}{2})$  and  $X(f + \frac{\alpha}{2})$ . SCD function can be expressed in terms of Fourier transform of CAF by using Wiener relation

$$S_x^\alpha(f) = \int_{-\infty}^{\infty} R_x^\alpha(\tau) e^{-i2\pi\alpha f \tau} d\tau, \quad (8)$$

this transform is called as the cyclic Wiener relation [12].

### 4. Test Environment

The test environment includes transmitter and receiver nodes. They will be described below.

#### 4.1. Transmitter Node

Using 4-quadrature amplitude modulation (QAM) mapping, bits are modulated by transmitter node. After the modulation process, pilot symbols using for channel estimation and synchronization is inserted as 4-QAM symbols. Then, serial data is divided into parallel data blocks. Zero padding symbols are inserted by using subcarrier allocation block. The subcarriers in time domain,  $x_{k,l}$  are obtained at the output of inverse discrete Fourier transform (IDFT) block as

$$x_{k,l} = \frac{1}{\sqrt{N}} \text{IDFT}[X_{n,l}] = \sum_{n=0}^{N-1} X_{n,l} e^{\frac{i2\pi kn}{N}} \quad (9)$$

where,  $X_{n,l}$  is the complex signal assigned to the  $n^{th}$  subcarrier of  $l^{th}$  OFDMA symbol. Then, CP is inserted to protect the signal from multipath channel effects after conversion to serial data. In the time domain,  $L$  symbols of CP are copied to the beginning of the frame. The analog waveform  $s_{k,l}(t)$  are obtained from OFDMA symbols. It is shown that

$$s_{k,l}(t) = \sum_{t=0}^{\infty} x_{k,l} \frac{1}{T-T_{CP}} e^{i2\pi(t-lT-T_{CP})\frac{w}{N}} \quad (10)$$

by using rectangular pulse with carrier frequency  $kW/N$  and  $T$  and  $T_{CP}$  are the total duration of transmission and duration of CP part, respectively. Used transmitter structure is given in Figure 1.

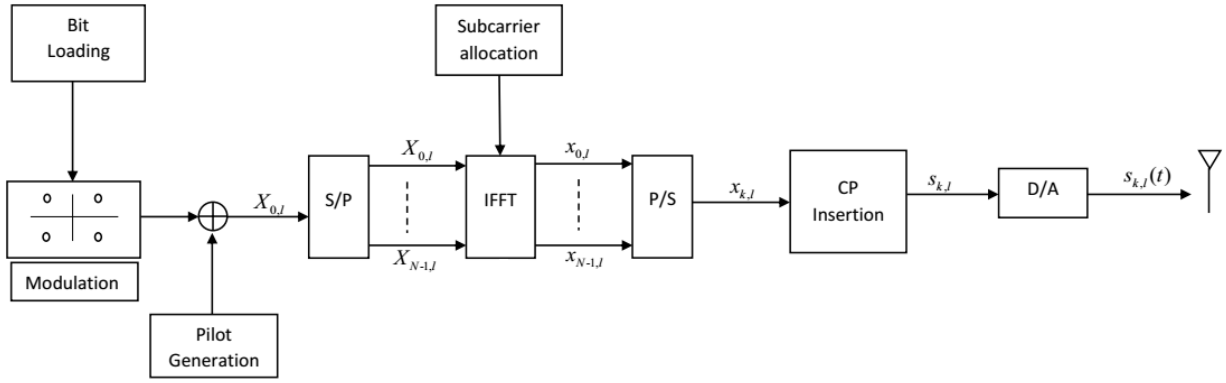


Figure 1. OFDMA transmitter block diagram

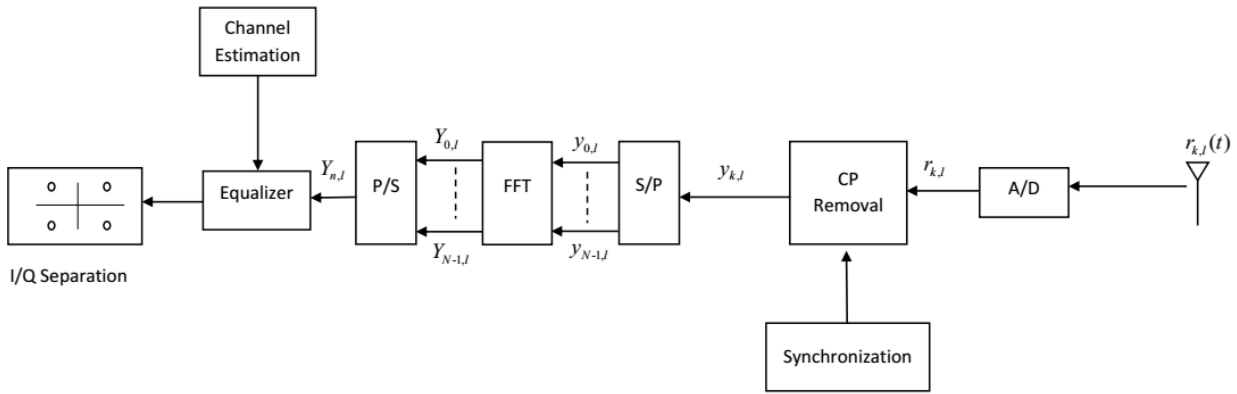


Figure 2. OFDMA receiver block diagram

**4.2. Receiver Node**

Received RF signal is digitalized by using analog to digital converter block. The output of this block can be denoted with  $r_{k,l}$ . CP part of symbols appending at the transmitter side is removed. After removal process, time domain symbols  $y_{k,l}$  are divided into parallel data blocks by using DFT block. The signal  $Y_{n,l}$  is obtained as,

$$Y_{n,l} = \text{DFT}[y_{k,l}] = \frac{1}{\sqrt{N}} \sum_{n=0}^{N-1} y_{k,l} e^{-\frac{j2\pi kn}{N}} \quad (11)$$

in the frequency domain. The symbols are converted to serial data. The least square method is employed for pilot based channel estimation. For every 8 data subcarriers, one pilot subcarrier and zero forcing equalization are used. Employed receiver structure is given in Figure 2.

**4.3. Testbed Properties**

The real time measurement setup includes two NI USRP 2921 nodes as a transmitter and NI PXI 1082 node as a receiver. The nodes used for transmission can operate in the 2.4-2.5 GHz and 4.9-5.9 GHz bandwidths. The node employed as receiver has RFSA module to analyze the

signal. Implemented testbed is programmed with NI-LabVIEW which is used for system design.

To overcome synchronization problem in OFDMA system, NI PXI 6683 timing and synchronization module is employed for 10 MHz clock signal. For synchronization in the software side, NI RFSG signal and clocking generation software and NI LabVIEW are used. In order to design an accurate system, time and frequency offset algorithms in [13] are used. Hardware and test environment are shown in Figure 3. NI USRP 2921 transmitters are placed in setup. The transmitters are located at 20 cm and 40 cm away from receiver NI PXI 1082 for user-1 and user-2, respectively. This difference provides asymmetric data transmission.

OFDMA transmitter nodes are designed respect to parameters given in Table 1. Moreover, PHY parameters of OFDMA system measurements are given in Table 2. These parameters are configured by using Virtual Instruments (VIs) which coordinate hardware and software. For  $N = 128$  subcarriers, 4-QAM symbols are generated by loading 72 bits into the system. Using pseudonoise sequence, pilot symbols which are modulated by using 4-QAM symbols, are generated. Array functions in LabVIEW are employed for pilot symbols and subcarrier distribution functions. 56 subcarriers are used as zero padding for guard subcarrier. CP lengths are kept the same for user-1 and user-2.

The receiver side of OFDMA system is set by using RFSA and VIs. It is operating at 2.45 GHz carrier

frequency with 1MS/s. Aforementioned functionalities such as CP removal, zero padding removal, pilot and data

**Table 1.** OFDMA frame structure with  $N = 128$  subcarriers

Configuration	Zero Padding	Pilot + Information	DC Component	Pilot + Information	Zero Padding
Subcarrier Index	0-27	28-63	64	65-100	101-127
User 1	28 Subcarriers	36 Subcarriers	1 Subcarrier	36 Subcarriers as ZP	27 Subcarriers
User 2	28 Subcarriers	36 Subcarriers as ZP	1 Subcarrier	36 Subcarriers	27 Subcarriers

**Table 2.** PHY properties of OFDMA based system measurements for two users

System Parameters	User1 / User2
Carrier Frequency	2.45 GHz
I/Q Data Rate	1 MS/sec
Transmission Bandwidth	1.25 MHz
Number of Bits used in One Frame	72 bits
Number of 4-QAM Symbols	36 subcarrier
Number of Pilot Subcarriers	4
Number of Information Subcarriers	32
Zero Padding Length (including DC)	56
IFFT/FFT Length ( $N$ )	128

decomposition are handled by using array functions. Besides array functions, channel estimation based on linear interpolation and zero forcing equalization are used. I/Q data of the whole measurement are logged at the receiver node to process.

### 5. Measurement Results

The logged data is processed and the measurement results are detailed below.

#### 5.1. Communication Performance Related Measurements

Firstly, we mention about the received OFDMA signal related measurements. The measurement results are obtained for both users' transmit data. At the receiver side, both users' data can be differentiated from each other. The constellation diagrams for received signals are given in Figure 4 and Figure 5. Figure 4 denotes the constellation diagram for user-1 received signals with

$N = 128$  subcarriers and CP length  $L = 16$ . Figure 5 shows the constellation diagram for user-2 received signals with the same parameters.

Using CP, time and frequency offsets can be corrected. Furthermore, the use of CP can aid combat

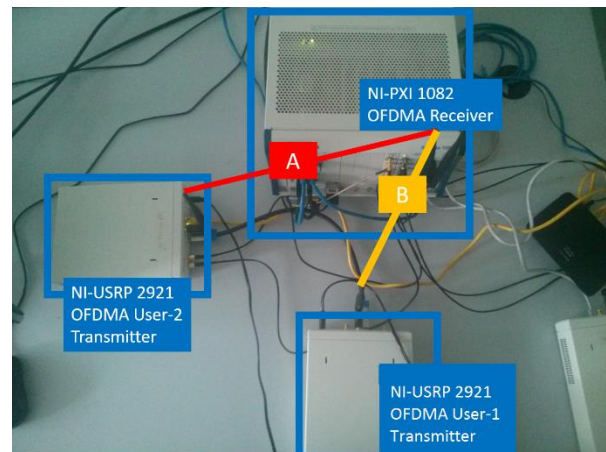


**Figure 3.** NI USRP 2921 nodes are used for OFDMA transmitter nodes. NI PXI 1082 module is used for receiver node, clocking, and synchronization. For asymmetric transmission, the distance A is set as 40 cm and the distance B is 20 cm.

the multipath delay spread. For various CP lengths, the EVM performances of both users are measured and given Figure 6. For CP lengths longer than 32, the EVM the performance of received signal gets worse because of the sensitivity of OFDMA system to CP. When CP length changes from 32 to 64, EVM measurement is increasing by 430.72% for user-1. As there is an asymmetry based on distance difference, the received signals have varying EVM performance.

#### 5.2. Measurement about Cyclostationarity of OFDMA Signals

OFDMA signals consist of hidden repeated patterns. Therefore OFDMA signals can be differentiated from each other by using their features like various CP lengths although they use same protocols.

We investigate whether we can identify the signals belonging to different users even though they have the same CP length. Thus, CAF measurements of OFDMA signals with the same CP length are performed by using various time delays ( $\tau$ ) and cyclic frequencies ( $\alpha$ ). Due to the position of zero padding in the frame structure and random distribution of data symbols, it is expected that there will be differences between the CAF of the signals and also SCD functions of the signals. CAFs of the signals are given in Figure 7 and Figure 8 for user-1 and user-2, respectively.

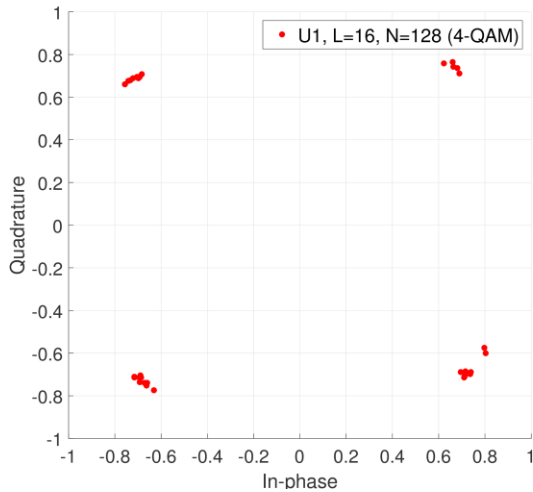


Figure 4. Constellation diagram for user-1 received signal with  $N = 128$  and  $L = 16$

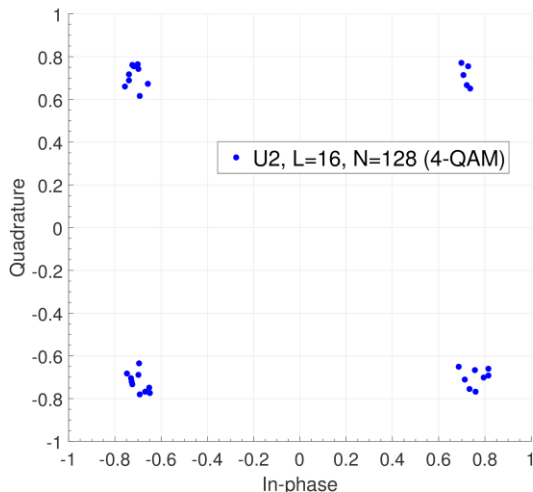


Figure 5. Constellation diagram for user-2 received signal with  $N = 128$  and  $L = 16$

It is not trivial to differentiate the figures, so to focus on their differences, the normalized CAF measurements of both users' OFDMA signal at a constant lag of time with 128 subcarriers and CP length of 16 are shown in Figure 9. It is clearly seen from the figure that user-1 and user-2 signals have different CAF values because of different zero padding locations in frame and random distribution of bits. Since the OFDMA signals have the

same CP length, the peak values appear at almost the same cyclic frequencies. However, there are small differences in the CAF values of the two signals due to zero padding and random bit distribution. Using these differences, the signals can be differentiated even if they have the same CP length.

In communication systems, the frequency domain is widely used. Hence, SCD function behavior is investigated to observe how CAFs change in the frequency domain. SCD functions of OFDMA signals belonging user-1 and user-2 are given in Figure 10 and Figure 11, respectively. The differences between SCD

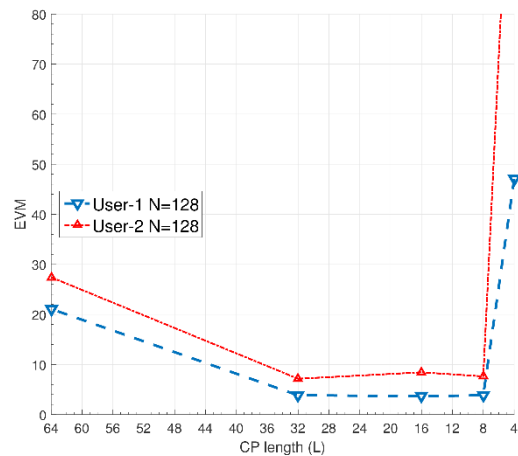


Figure 6. EVM performance for different CP lengths ( $L$ ) can be detected. Then, countermeasures can be resorted in order to avoid unauthorized spectrum usage.

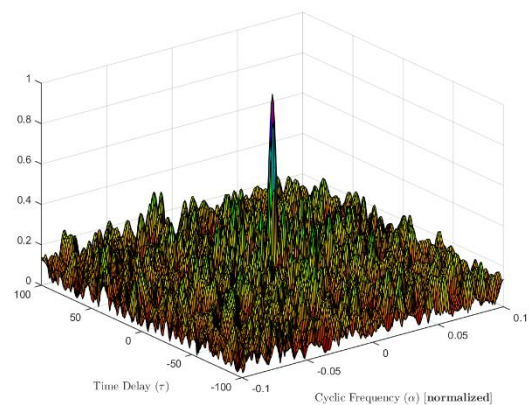
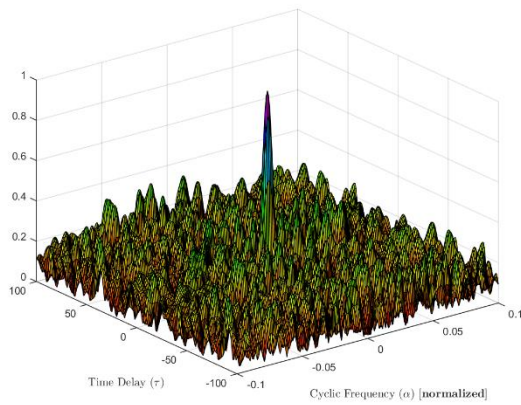


Figure 7. CAF of user-1 for different time delays and cyclic frequencies





**Figure 8.** CAF of user-2 for different time delays and cyclic frequencies

functions of both OFDMA signals can be seen easily. Using these visible differences, the OFDMA signals of different users can be blindly differentiated. Following this, the

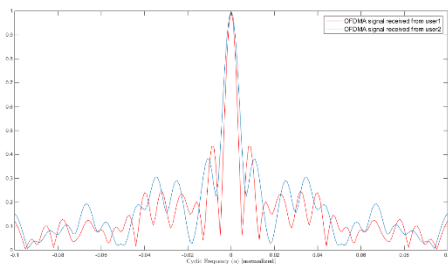


**Figure 9.** Normalized CAF of both users with the same CP length  $L = 16$  and a constant time lag for  $N = 128$

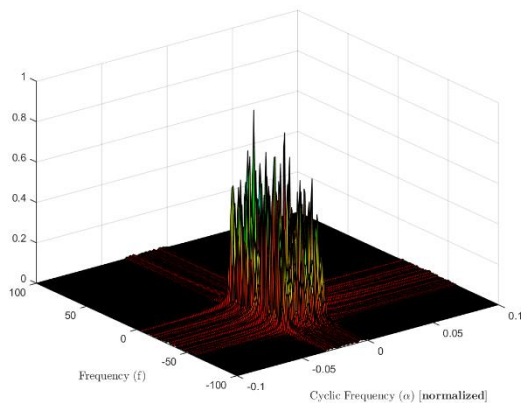


**Figure 10.** SCD function of user-1 for different time delays and cyclic frequencies

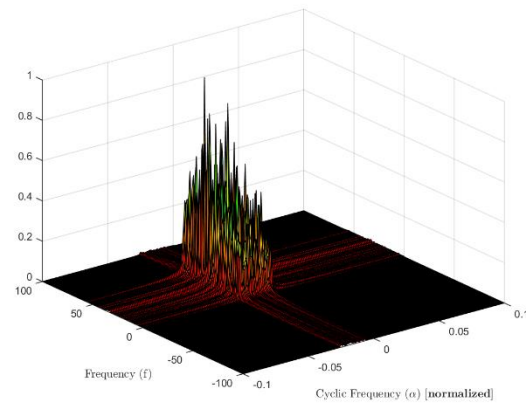


**Figure 11.** SCD function of user-2 for different time delays and cyclic frequencies

frequency occupancy of any unauthorized user can be detected. Then, countermeasures can be resorted in order to avoid unauthorized spectrum usage.

## 6. Conclusion

In this paper, cyclostationarity signal analysis is used to determine how zero padding position affects the signal characteristics. As a consequence, the differences due to zero padding position in a frame enable to differentiate OFDMA signals received from different users. SDR based measurement results are captured with the designed testbed. CAF and SCD functions are computed for each signal transmitted by each user. Differences between this cyclostationary features are highlighted. Using cyclostationary features, blind identification can be realized for interfering signals even if it has the same CP length. Given expressions can be used to differentiate signals received from users by using classifiers.

## 7. References

- [1] K. Tekbiyik, H. Alakoca, H. B. Tuğrel, C. Ayyıldız, and G. K. Kurt, "Identification of OFDM Signals using Cyclic Autocorrelation Function," in National Conference on Electrical, Electronics and Biomedical Engineering (ELECO), 2016, pp. 622–626.
- [2] A. Fehske, J. Gaeddert, and J. H. Reed, "A New Approach to Signal Classification using Spectral Correlation and Neural Networks," in First IEEE International Symposium on New Frontiers in Dynamic Spectrum Access Networks (DySPAN), 2005, pp. 144–150.
- [3] M. Davy, A. Gretton, A. Doucet, P. J. Rayner et al., "Optimized Support Vector Machines for Nonstationary Signal Classification," IEEE Signal Processing Letters, vol. 9, no. 12, pp. 442–445, 2002.
- [4] G. Huang and J. K. Tugnait, "On Cyclostationarity Based Spectrum Sensing under Uncertain Gaussian Noise," IEEE Transactions on Signal Processing, vol. 61, no. 8, pp. 2042–2054, 2013.
- [5] C. Du, H. Zeng, W. Lou, and Y. T. Hou, "On Cyclostationary Analysis of WiFi Signals for Direction Estimation," in IEEE International Conference on Communications (ICC), 2015, pp. 3557–3561.

- [6] R. Zhou, X. Li, T. Yang, Z. Liu, and Z. Wu, "Real-time Cyclostationary Analysis for Cognitive Radio via Software Defined Radio," in Global Communications Conference (GLOBECOM), 2012, pp. 1495–1500.
- [7] Q. Yuan, P. Tao, W. Wenbo, and Q. Rongrong, "Cyclostationarity based Spectrum Sensing for Wideband Cognitive Radio," in IEEE International Conference on Communications and Mobile Computing, vol. 1, 2009, pp. 107–111.
- [8] S. Ma, C. Zhao, and Y. Wang, "Fractional Low Order Cyclostationary Spectrum Sensing Based on Eigenvalue Matrix in Alpha-stable Distribution Noise," in First International Conference on Pervasive Computing Signal Processing and Applications (PCSPA), 2010, pp. 500–503.
- [9] A. Al-Dulaimi, N. Radhi, and H. Al-Raweshidy, "Cyclostationary Detection of Undefined Secondary Users," in Next Generation Mobile Applications, Services and Technologies, 2009, pp. 230–233.
- [10] W. A. Brown and H. H. Loomis, "Digital Implementations of Spectral Correlation Analyzers," IEEE Transactions on Signal Processing, vol. 41, no. 2, pp. 703–720, 1993.
- [11] H. B. Tuğrel, H. Alakoca, K. Tekbiyik, G. K. Kurt, and C. Ayyıldız, "OFDMA System Identification using Cyclic Autocorrelation Function: A Software Defined Radio Testbed," in 10th International Conference on Signal Processing and Communication Systems (ICSPCS), 2016, pp. 1–7.
- [12] W. A. Gardner, "Exploitation of Spectral Redundancy in Cyclostationary Signals," Signal Processing Magazine, IEEE, vol. 8, no. 2, pp. 14–36, 1991.
- [13] J.-J. Van de Beek, M. Sandell, P. O. Borjesson et al., "ML Estimation of Time and Frequency Offset in OFDM Systems," IEEE Transactions on Signal Processing, vol. 45, no. 7, pp. 1800–1805, 1997.



**Kürşat Tekbiyik** was born in Erzincan, Turkey. He graduated from IMKB Nevzat AYAZ Science High School, Erzincan. Currently, he is working towards his B.S degree at Istanbul Technical University, Istanbul, Turkey. He is presently employed at Wireless Communication Research Laboratory, Istanbul Technical University. His research interests include signal identification, cyclostationarity

signal analysis in wireless communication systems.



**Hakan Alakoca** was born in Aydin, Turkey. He received the B.Eng. degree in telecommunication engineering from the Istanbul Technical University, Istanbul, Turkey, in 2016. He is M.Sc. candidate in applied informatics from the Istanbul Technical University, Institute of Informatics, Istanbul, Turkey. He is member of wireless communication research labs in Istanbul Technical University. His current research interests are physical layer security,

LTE based cellular systems optimizations, software defined radios and wireless testbeds.



**Halim Bahadır Tuğrel** was born in Bursa, Turkey. He received the B.Eng. degree in electronics and telecommunication engineering from the Istanbul Technical University, Istanbul, Turkey, in 2015. He is M.Sc candidate in telecommunication engineering from the Istanbul Technical University, Institute of Science, Istanbul, Turkey. He is member of wireless communication research

and Radio-Frequency electronics labs in Istanbul Technical University. His current research interests are communication electronics circuits, IoT, localization and tracking problems, physical layer security, LTE based cellular systems, software defined radios and wireless testbeds.



**Cem Ayyıldız** received the B.S. degree in electronics and electrical engineering from Middle East Technical University, Ankara, Turkey, in 2006 and the M.Sc. degree in micro-electronics engineering from the University of Applied Sciences Bremen, Germany in 2008. From 2008 to 2010, he has worked in defense industry on communication systems. Since 2010, he is the leading hardware engineer in Turkcell R&D Applied Research and Technology. He is a

member of Steering Technical Group of ITEA since 2015. Currently, he is developing localization algorithms for wireless systems that could be used for security purposes.



**Assoc. Prof. Güneş Karabulut Kurt** received the B.S. degree (with honors) in electronics and electrical engineering from Bogazici University, Istanbul, Turkey, in 2000 and the M.A.Sc. and Ph.D. degrees in electrical engineering from the University of Ottawa, Ottawa, ON, Canada, in 2002 and 2006,

member of the COST Action 1104.

respectively. From 2000 to 2005, she was a Research Assistant with the CASP Group, University of Ottawa. Between 2005 and 2006, she was with TenXc Wireless, where she worked on location estimation and radio frequency identification systems. From 2006 to 2008, she was with Edgewater Computer Systems Inc., where she worked on high-bandwidth networking in aircraft and priority-based signaling methodologies. From 2008 to 2010, she was with Turkcell R&D Applied Research and Technology, Istanbul. Since 2010, she has been with Istanbul Technical University, where she is currently an Associate Professor. Dr. Karabulut Kurt is a Marie Curie Fellow and her project REALMARS is selected to be a success story by European Commission Research Executive Agency. She is the author of numerous publications and 7 international patents. Dr. Karabulut was involved in various research projects including STREP, EUREKA and ITEA-2 projects on wireless networks. She is a management committee





